Vol. 48: 107–121, 2022
https://doi.org/10.3354/esr01190

ENDANGERED SPECIES RESEARCH
Endang Species Res

Published July 7[§]

High annual survival suggested by size structure of Kemp's ridley sea turtles captured by coastal research trawling in the Northwest Atlantic Ocean since 1990

Michael D. Arendt[*], R. Pearse Webster, Jeffrey A. Schwenter

Marine Resources Division, South Carolina Department of Natural Resources, 217 Fort Johnson Road, Charleston, South Carolina 29412, USA

ABSTRACT: Abundance of Kemp's ridley sea turtle *Lepidochelys kempii* Garman, 1880 in the Northwest Atlantic Ocean (NWA) is far less than in the Gulf of Mexico (GOM), but encounters of this species in the NWA have increased in recent decades. Consequently, improved opportunity exists to evaluate population structure, which is of particular interest given suggestions of renewed decline in annual survival rates in the GOM. Here we use size structure for Kemp's ridley sea turtles captured (n = 617) by research trawling in the South Atlantic Bight (SAB) to assess survival since 1990 following age assignment using recently published size-at-age keys. With limited exception, the ratio of older (≥age 10) to younger (ages 1 to 9) sea turtles captured randomly was overwhelmingly stable and best aligned with high (≥0.9) annual neritic survival in theoretical models with fixed annual hatchling (*H*) recruitment. When annual *H* recruitment reflected exponential increase in *H* production since 1985, following low and generally stable production between 1966 and 1984, reduced *H* emigration proportion from the GOM to NWA and further increase in annual neritic survival were required to achieve the size/age structure reported for in-water data. Stepwise regression using monthly values for 5 climate indices simulated (adj. r^2 = 0.77) proportionate annual *H* decline, which better explained observed survey size/age structure than climate-based prediction (adj. r^2 = 1.00) of published particle emigration rates. Temporal decline in proportionate *H* recruitment to the NWA should increase retention of juveniles in the GOM to further enhance multi-generational population rebuilding.

KEY WORDS: Age · Marine turtles · North Atlantic · Population dynamics · Recruitment

---

1. INTRODUCTION

Comprehending the distribution, abundance, and demographic dynamics of any species is essential for evaluating temporal change and in turn fostering effective resource management. Consistent with the abundant-center hypothesis (Sagarin et al. 2006), monitoring surveys and corresponding conservation efforts often target epicenters of species distribution or abundance. Unfortunately, strict conformity to this sampling design disregards ecological variability that perpetuates plasticity in phenological responses within species ranges (Sagarin et al. 2006). Consequently, the 'conservation of both central and marginal populations' is now recognized as being 'equally important considerations in making management decisions' (Guo et al. 2005, p. 47). Among species globally listed as 'Critically Endangered' by the International Union for Conservation of Nature and Natural Resources (IUCN), the Kemp's ridley sea turtle *Lepidochelys kempii* Garman, 1880 has spatially restricted nesting which, in turn, has fostered a belief that foraging grounds far removed from that epicenter are of fringe population value.

The Kemp's ridley sea turtle is the most recently described of 7 extant sea turtle species, with the type

---

[*]Corresponding author: arendtmd@dnr.sc.gov

[§]Corrections were made after publication. For details see www.int-res.com/abstracts/esr/v48/c_p107-121/
This corrected version: July 18, 2022

Publisher: Inter-Research · www.int-res.com

specimen, first thought to be a hybrid, curated from the southeastern Gulf of Mexico (GOM) near Key West, Florida (Carr 1956). Extensive research and monitoring in recent decades establish the paramount importance of the western GOM due to spatial concentration of nesting (NMFS & USFWS 2015). Fidelity to seasonal foraging grounds throughout the GOM basin is also known from telemetry studies conducted with both juveniles and adults (Schmid et al. 2003, Schmid & Witzell 2006, Seney & Landry 2011, Shaver et al. 2016, Coleman et al. 2017, Gredzens & Shaver 2020). Although pockets of aggregation occur in the eastern GOM (Hart et al. 2018, Fujisaki et al. 2020), occurrence in this region is most common in winter, at southernmost latitudes, and episodic in nature (Renaud & Williams 2005).

Despite the understandably GOM-centric view of Kemp's ridley life history, there is merit to historical reference of this species as the Atlantic ridley (Coker 1906, Hardy 1962). Distribution along the US eastern seaboard spans nearly 20° of latitude, and importance of the Northwest Atlantic Ocean (NWA) as developmental habitat is founded (Morreale & Standora 2005). Hatchlings also occur episodically as far east as the Mediterranean Sea (Manzella et al. 1988, Carreras et al. 2014), even during some low hatchling production years (NMFS & USFWS 2015). Along the US east coast, movements between the mid-Atlantic (MAB) and the South Atlantic (SAB) Bights, documented from tag-recapture and satellite telemetry, correspond with seasonal water temperature changes (Henwood & Ogren 1987, Schmid 1996, Morreale 1999). Similar to the eastern GOM, seasonal occurrence of Kemp's ridley sea turtles at the southernmost latitudes of the NWA distribution range is most common in winter (Renaud 1995, Gitschlag 1996).

Pritchard (1969, p. 13) initially described hatchling dispersals 'outside of the Americas' as 'presumably lost for ever (sic) from the breeding population' and nearly 4 decades later noted that 'debate continues as to whether the animals in the U.S. Atlantic waters, especially in the northern section, are lost to the population or are indulging in a normal (or at least optional) part of their developmental odyssey' (Pritchard 2007, p. 52). Although Carr (1980) and Hendrickson (1980) were receptive to the notion that Kemp's ridley sea turtles could return to the GOM, because few individuals tagged in the NWA are re-sighted in the GOM (see review by Caillouet et al. 2015), most emigration out of the GOM largely remains regarded as retarding reproductive recruitment (Caillouet 2019, Caillouet & Gallaway 2020). Adult sizes occur in the NWA (Avens et al. 2020), but given limited nesting outside of the GOM, NWA Kemp's ridley sea turtles are predominately prized as predator or prey (Caillouet & Gallaway 2020). Increased Kemp's ridley sea turtle nesting in the SAB since 2015, notably in NC (NCWRC unpubl. data, http://seaturtle.org/nestdb/?view=1) succeeds increased neritic occurrence in the region (Braun McNeill et al. 2018) and suggests far greater ecological value than historically credited. As such, although present SAB nesting pales in comparison with even tertiary level colonies in the western GOM, the idea that a SAB colony could contribute to recovery is at least being considered (Caillouet & Gallaway 2020).

Renewed interest in the role of Kemp's ridley sea turtles in the NWA stems from oceanographic modeling that documents passive drift of upwards of 28% of simulated cohort particles from the GOM to the NWA annually (Putman et al. 2013). Revised models weighted for Kemp's ridley sea turtle hatchling production since 1966 also suggest substantial increase in oceanic and pelagic habitats in the NWA, particularly in the SAB (Putman et al. 2020a). Consequently, emigration to the NWA and potential population 'sink' loss for the GOM could exacerbate (Caillouet 2019, Caillouet & Gallaway 2020) deviation in annual nest counts from more optimistic predictions following more than a decade of apparent recovery through 2009 (Crowder & Heppell 2011). Therefore, the first objective of this study was to assess neritic assemblage structure by applying size-at-age data (Avens et al. 2020) to Kemp's ridley sea turtles captured in 2 multi-decadal coastal research trawl surveys in the SAB (Arendt et al. 2012a, Willis et al. 2015). Consistent with a call to evaluate temporal variability in age group structure (Caillouet 2019), for the second objective we used the inverse power equation to convert our age group quotient to an appropriate scale for elucidating the net effect of annual survival and potential change in neritic recruitment. For the third objective, we first used matrix modeling with fixed annual hatchling production across a broad spectrum of survival trajectories to identify a best general fit model to explain survey structure. Next, annual recruitment and survival were systematically manipulated to then identify the best 'real world' fit for annual hatchling production from the primary nesting beach since 1966 (NMFS & USFWS 2015). Following identification of the best fit dynamic model, temporal change in neritic abundance was projected, consistent with a call by Putman et al. (2020a) to validate model simulations where even high particle simulation densities represented <2 Kemp's ridley sea turtles per km^2.

2. MATERIALS AND METHODS

A glossary of terms is provided in Table A1 in the Appendix.

2.1. Survey operation and sea turtle capture and handling

Sea turtles were captured by research trawling in coastal (5 to 14 m deep) SAB waters (Fig. 1). Survey methodology nuances for each of the 2 primary data sources are described below, but all data were considered to evaluate potential sampling design impacts on (1) overall sample size and (2) proportionate size structure. Data were not analyzed to report temporal catch rate trends, a more traditional in-water analysis (Arendt et al. 2012a, Braun McNeill et al. 2018); thus, evaluation of size structure across survey designs with variable sampling effort was statistically sound.

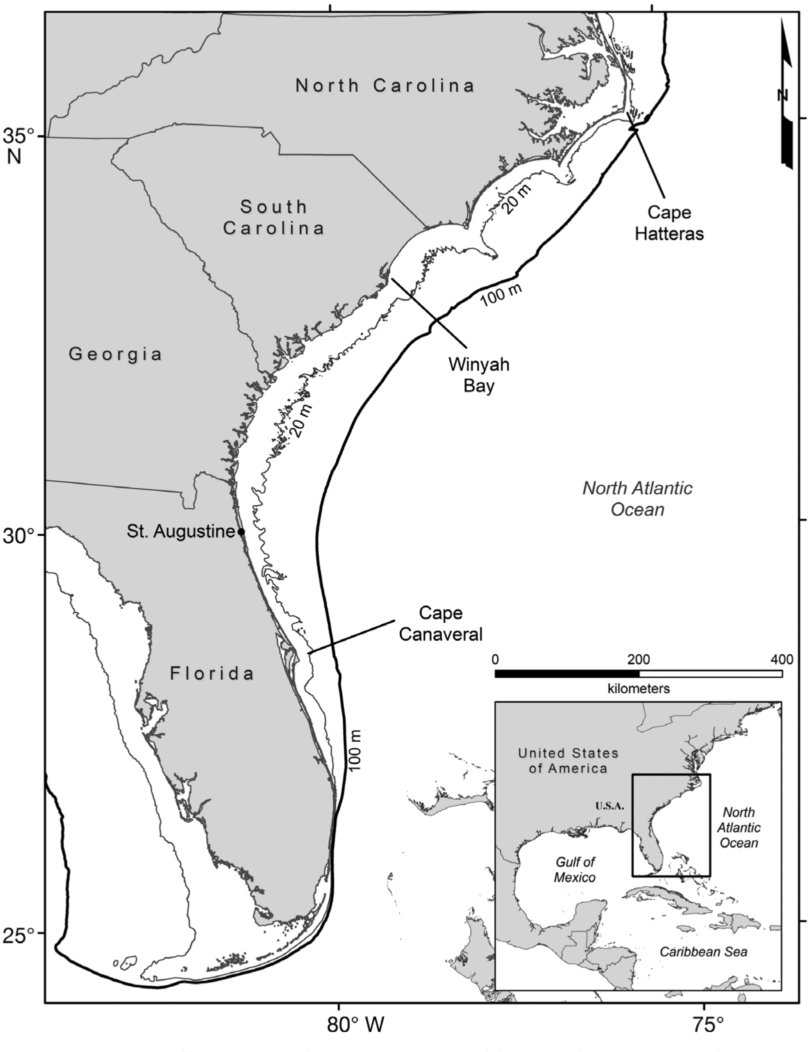

Fig. 1. Kemp's ridley sea turtles were captured by trawling in coastal waters (5–14 m deep) spanning the entirety of the South Atlantic Bight (SAB) from Cape Hatteras, NC, to Cape Canaveral, FL. The Southeast Area Monitoring and Assessment Program (South Atlantic) Coastal Trawl Survey (CTS) trawled from Cape Hatteras, NC, to Cape Canaveral, FL, between 1990 and 2019, and the Turtle Trawl Survey (TTS) trawled from Winyah Bay, SC, to St. Augustine, FL, beginning a decade later

The Coastal Trawl Survey (CTS) of the Southeast Area Monitoring and Assessment Program-South Atlantic (SEAMAP-SA) operated between Cape Hatteras, NC (35.2° N), and Cape Canaveral, FL (28.6° N), and sea turtle data collection began in 1990. The CTS operated during spring, summer, and fall seasons with a seasonal target of 78 to 112 stations, where stations represented all available options in station-limited areas (i.e. due to constrained bathymetry and/or seafloor ruggedness) or an annual subset of randomly selected stations from a larger station universe. For analyses, temporal subsets of the CTS were delineated to distinguish survey years (1) prior to the onset of a companion survey described below (CTS_1, 1990 to 1999), (2) concurrent with the companion survey through 2015 (CTS_2) to align with neritic assemblage modeling (see Section 2.4), and (3) for additional survey years after 2015 (CTS_3).

The In-Water Sea Turtle Trawl Survey (TTS) began in 2000 and was conducted within the central latitudes of the CTS between Winyah Bay, SC (33.1° N), and St. Augustine, FL (29.9° N). Annual sampling for the TTS only occurred in summer, and with the goal of maximum annual sampling of several hundred stations randomly selected from a list of >1500 possible locations. Consequent to stepwise increases in vessel sea day rates and reductions in operational funding, annual TTS station completion declined temporally but was never <100. Consistent with the CTS, survey years for the TTS were delineated in analyses to reflect correspondence with neritic assemblage modeling (TTS_1) and survey years completed after 2015 (TTS_2).

Non-random surveys were also completed during a subset of TTS survey years, including limited fishery-dependent monitoring aboard commercial shrimp vessels off Brunswick, GA, in

2000 (TTS_3) and off Charleston, SC during 2000 to 2003 (TTS_4). In lieu of broader coverage randomized surveys, fishery-independent trawling occurred in the shipping entrance channel to Charleston, SC, during 2004 to 2007 (Arendt et al. 2012b) and again in 2016 and 2017 (TTS_5). Likewise, to assess potential differences in Kemp's ridley sea turtle capture (and recapture) rates and size structure, repetitive trawling off Brunswick, GA, also occurred in 2016 and 2017 (TTS_6).

Two trawl nets were towed for the CTS (RV 'Lady Lisa') and the TTS (RVs 'Lady Lisa' and 'Georgia Bulldog'), but 4 nets were towed by fishery-dependent vessels (FVs 'Winds of Fortune' and 'Bounty' for Charleston, SC; 'Miss Savannah' for Brunswick, GA). Trawl net headrope length was 22.9 m for mongoose-type Falcon trawl (CTS_{1-3}), 18.3 m for flat nets ($TTS_{1-2,\ 5-6}$), and 12.2 m for fishery-dependent sampling (TTS_{3-4}). Throughout data collection, federal and state permits waived turtle excluder device (TED) requirements but reduced seafloor tow times to 20 min (CTS) or ≤30 min (TTS) to limit sea turtle drowning risk (Sasso & Epperly 2006). Trawling occurred during daylight hours with target towing speeds of 2.5 kn (CTS) and 2.8 kn (TTS); thus, targeted transect towing length spanned 1.5 km (CTS) to 2.6 km (TTS).

Sea turtles were removed from trawl net tail bags (or occasionally from the net body of larger mesh TTS nets) and visually and electronically scanned for pre-existing tags. Passive integrated transponder (PIT) tags (TX1406L or GPT-12, Biomark) were implanted near the base of the right front flipper (Wyneken et al. 2010). Inconel 681 metal tags issued by the University of Florida Cooperative Marine Turtle Tagging Program (CMTTP) were externally applied to the trailing edge of each front flipper of larger specimens. No within season recaptures occurred.

2.2. Sea turtle measurement and age assignment

A suite of morphometric measurements for all captured sea turtles was recorded as described by Bolten (1999); however, herein we analyze maximum straight-line carapace length (SCLnt), measured with calipers, to compare with Avens et al. (2020). For 3 TTS Kemp's ridley sea turtles with pre-existing posterior carapace injuries, SCLnt was estimated as [(0.9267 × SCW) + 3.9886; $r^2 = 0.98$] generated from maximum straight-line carapace width (SCW) for non-injured TTS captures. Likewise, SCLnt for 11 CTS sea turtles was estimated using a similar within-survey equation [SCLnt = (0.9222 × SCW) + 4.2417, $r^2 = 0.98$], but also using curved carapace width (CCW) for 5 additional CTS sea turtles [SCLnt = (0.9474 × CCW) + 0.5615 ($r^2 = 1.0$)]. Only minimum SCLnn was available for 2 CTS sea turtles, neither with carapace damage, and was used as a proxy for SCLnt for age assignment.

SCLnt was used to assign an age based on the closest absolute spline mean size predicted from generalized additive mixed models for the NWA per Table 4 of Avens et al. (2020). Kemp's ridley sea turtles <21.2 cm SCLnt, the smallest spline mean size reported by Avens et al. (2020), were assigned as age 1. Likewise, for Kemp's ridley sea turtles >64.7 cm SCLnt, the maximum mean spline size in Avens et al. (2020), continued annual increases of 0.2 cm were used to extend the distribution for ages >20. Chi-square analysis (Minitab 20; Minitab) revealed no significant difference ($p > 0.05$) in the proportion of 2 age groups (<10, ≥10) with respect to capture season or spatial capture (NC, SC, GA, FL) for CTS captures; thus, only analysis among temporal delineations previously described were considered further. Chi-square analysis was also used to test for differences in estimated age structure between CTS and TTS data across 3 age groups: A0 to A2; A3 to A9; and ≥A10.

2.3. Age group structure variability across surveys and designs

Based on concern that high juvenile abundance could be adversely affecting nesting trends in the GOM due to density-dependent limitations for adult foraging, Caillouet (2019) encouraged evaluation of temporal change in the quotient (Q) of older to younger Kemp's ridley sea turtles. When annual recruitment remains constant, annual survival (S) solely determines Q and can be solved for using the inverse power equation [$S = Q^{(1/t)}$] where 't' in the exponent term denotes the time interval between age groups. This relationship is the backbone of 'cross-sectional' and 'longitudinal' catch curve estimation used to compute survival in various fisheries since 1913 (see Hoenig & Gedamke 2007), as well as to derive survival for Kemp's ridley nest count modeling in the GOM (Heppell et al. 2005). In stark contrast to mark-recapture methods which require physical re-encounter of a reasonably large subset of specimens to estimate annual survival, 100% of survey captured specimens should inform catch curve analysis.

Annual recruitment (R) is rarely stable in ecological systems and thus also influences Q, and depending on the extent of temporal change, could be at least as important an influence on Q as annual survival. Therefore, both R and S were embraced herein and reported as a neritic survival equivalent (NSE) score [NSE = $Q^{(1/t)}$]. Longer t provides greater sensitivity because (1) higher survival is necessary to retain a higher proportion of older animals and (2) the asymptotic nature of the inverse power equation introduces less interpretative bias. Therefore, to ensure that t minimally influenced NSE scores, ages 1 to 9 were compared to ages 10 to 34, with a mean age group difference (t) of 17; this also scaled NSE to the magnitude of annual survival rates pertinent to population modeling. Age 1 corresponds to the youngest neritic recruits reported by Avens et al. (2020). Age 10 approximates sexual maturity for Kemp's ridley sea turtles in the GOM but not in the NWA (Avens et al. 2020); however, survival requirements to reach age 10 transcend geography. Terminal age 34 was slightly older than the oldest age (30.25) reported by Avens et al. (2020), but as noted by Gallaway et al. (2016), terminal model age includes all survivors that age and older. Age 34 also projected the 1966 cohort, the start of annual hatchling (H) data (NMFS & USFWS 2015), to the TTS start.

2.4. Neritic assemblage matrix modeling

Twenty-seven theoretical neritic assemblages (TNAs) were generated in Microsoft (MS) Excel 2016 (Microsoft Corp.) by multiplying fixed annual H abundance (5440; ~16% of mean 1966 to 1984 H) by age 0 (A0) survival to generate abundance (integer), then repeated with age-specific survival rates. Survival rates reflected combinations of low, medium, and high values for each of 3 life history stages (ages 0 to 2, ages 3 to 5, and ages 6+ yr), which also encompassed the wide range of survival values suggested since 1988 for these age groups (NMFS & USFWS 2015). Age group delineations also corresponded with nest count modeling for the GOM (Heppell et al. 2005). Annual survival of ages A0 to A2 was assumed to improve with increasing transition to neritic vs. oceanic habitats (Avens et al. 2020); thus, the following 3 A0–A1–A2 scenarios were considered: 0.15–0.18–0.27 to 0.35–0.38–0.47 to 0.55–0.58–0.67. For initial neritic distribution (ages A3 to A5), annual survival rates were 0.3, 0.5, or 0.7. For neritic distribution beginning at age A6, annual survival rates were 0.7, 0.8, or 0.9. Cluster analysis (Minitab^{20}) was then used to describe associations between age-based survival rates and TNA, NSE, and Q where the latter was expressed as the percent of the TNA represented by animals ages 10 to 34 yr.

To explore interactions between variable annual H recruitment and age-based survival, matrix modeling was used to project neritic assemblage structure for known annual H production during 1966–2014 (NMFS & USFWS 2015). Assemblage projection was achieved using multiple, interactive worksheets contained within a single MS Excel file. The first sheet featured the age-specific annual survival rates of the least conservative TNA schedule that generated the lowest absolute NSE difference with CTS_2 and TTS_1 data. The first sheet also included annual H production since 1966. For cohorts older than 1966, creation of a 'burn-in' age structure required several steps. First, annual nest counts in 1966 (n = 5991) were divided by clutch frequency (2.5) then multiplied by remigration interval (2) values used for nest count modeling (Heppell et al. 2005) to approximate the 1966 adult female population. Per in-water sex ratios (Witzell et al. 2005), we divided total adult females by 0.7 to generate an estimate of all adults in 1966 (n = 6845), presumably all at least age A10. H abundance was then systematically varied until the best fit TNA survival schedule produced a sum of age A10 to A34 as close as possible (n = 6850) to the predicted abundance in 1966. Lastly, given simulated annual emigration rates from the GOM to the NWA of 4 to 28% (Putman et al. 2013), we assumed 15% of each age (A1 to A34) for the 1966 NWA 'burn in'.

The second sheet calculated annualized cohort persistence and was computed by diagonally populating the initial calculation using the 'offset' function and then routine multiplication thereafter through age A34 (i.e. age 1 proportion = age 0 proportion × age 1 survival, etc.). The proportion of each cohort remaining in year 'x' was then multiplied by initial cohort abundance to generate an integer count of annual abundance for each age (A1 to A34). Survival schedules for different model configurations were archived as unique sheets so that only the sheet name needed to be changed in the computational formulas to update the model output. The 'offset' function was again used to tally annual age group (A1–A9, A10–A34) abundances. For analysis, temporal comparisons were restricted to 1990 (i.e. earliest CTS data) through 2015 (i.e. maximum age 1 projection with terminal H in 2014; NMFS & USFWS 2015).

Given a multitude of potential configurations, modeling was selectively and systematically performed to evaluate dynamic H recruitment proportion and survival trajectories (see Table 4). Across model configurations, we adhered to conventional wisdom that

NWA Kemp's ridleys predominantly remained in this system vs. permanently returning to the GOM; if this were not the case, *Q* and NSE in all model configurations would be subsequently reduced. To ensure no matrix coding errors, annual *H* input was first fixed at 5100 (model M1) which approximated 15% annual emigration from the GOM to the NWA between 1966 and 1985, and in turn provided reference for exponential increase in annual *H* production after 1985. Next, annual survival values were fixed at a single TNA schedule to assess the impact of annual *H* recruitment from the GOM to the NWA for 3 broad trajectories: fixed (0.15) proportion of 1966 to 2014 *H* production (model M2); annual *H* proportion decrease (from 0.28 in 1966 to 0.04 in 2014, model M3); and annual *H* proportion increase (from 0.04 in 1966 to 0.28 in 2014, model M4). Subsequent model configurations only considered the annual *H* recruitment schedule among models M2 to M4 with the least different (from CTS and TTS) NSE score. Model M5 also included a smooth decline (i.e. 0.002 annually) in survival for ages A0 to A2 from 0.660 (1966) to 0.538 (2015); this produced a mean annual survival of 0.60, the same as mean annual survival for these ages in models M1 through M4. Model M6 built on model M5 by including a smooth increase (i.e. 0.002 annually) in survival for ages A3 to A5 (0.452 in 1966, 0.550 in 2014) and ages A6 to A34 (0.852 in 1966, 0.950 in 2014) which produced the same mean annual survivals for these age groups as models M1 to M4. The next 2 models (M7, M8) built on models M4 and M5, respectively, by fixing age A3 to A5 survival at 0.7 annually.

2.5. Annual emigration rate associations

After identification of a general *H* recruitment trajectory best aligned with CTS and TTS NSE, potential association with climate was explored. Given the importance of *Sargassum* sp. as a developmental habitat for oceanic sea turtle species (Witherington et al. 2012), we considered multiple climate indices known to influence the retention of this important macroalgae in the western GOM (Sanchez-Rubio et al. 2018). Monthly (standard) unsmoothed, long-format series of the Atlantic Multidecadal Oscillation (AMO) since 1856 (https://psl.noaa.gov/data/correlation/amon.us.long.data, accessed 30 July 2020) and monthly Atlantic Meridional Mode sea surface temperature (AMMs) and wind (AMMw) since 1948 were obtained from the NOAA Physical Sciences Library https://psl.noaa.gov/data/timeseries/monthly/AMM/, accessed 30 September 2021). Monthly North Atlantic Oscillation (NAO) and running tri-monthly El Niño Southern Oscillation (ENSO) values since 1950 were obtained (accessed 30 September 2021) from the Climate Prediction Center of the NOAA National Weather Service: www.cpc.ncep.noaa.gov/products/precip/CWlink/pna/nao.shtml; www.cpc.ncep.noaa.gov/products/analysis_monitoring/ensostuff/ensoyears.shtml).

Stepwise regression (Minitab^{20}, entry $\alpha = 0.05$) computed a best fit equation between monthly climate values and temporal decline in proportionate *H* recruitment C eq. A second stepwise regression equation (entry $\alpha = 0.5$, P eq.) reproduced particle emigration rates (2003 to 2010) predicted by Putman et al. (2013). Both equations were evaluated with fixed age A0 to A2 annual survival (models M9 and M12), with A0 to A2 survival negatively correlated with proportionate *H* recruitment (models M10 and M13), and with age A3 to A5 survival positively correlated with proportionate *H* recruitment (models M11 and M14). For the model configuration with least net difference between predicted and observed NSE scores, annual assemblage abundance was projected at multi- (1990–99, 2000–03, 2004–07, 2008–09) and annual (2010 to 2015) intervals selected to ensure that NSE was computed using a minimum of 10 Kemp's ridley sea turtles.

3. RESULTS

Beginning in 1990 (CTS) and 2000 (TTS) and through 2019, 617 Kemp's ridley sea turtles were captured by the CTS (n = 223, 36%) and the TTS (n = 394, 64%), respectively. Both surveys captured Kemp's ridley sea turtles small enough to be classi-

Table 1. Estimated age structure (from size distribution) of Kemp's ridley sea turtles captured by research trawling surveys in the South Atlantic Bight 1990–2019 (Coastal Trawl Survey, CTS) or 2000–2019 (Turtle Trawl Survey, TTS). SCLnt: straight-line carapace length; n: no. of turtles captured

Assigned age (yr)	TTS (n)	%	SCLnt (cm)	CTS (n)	%	SCLnt (cm)
1	5	1	16.3–23.9	2	1	22.8–22.9
2	15	4	24.3–27.7	9	4	24.0–27.3
3–9	313	79	27.8–52.6	175	78	27.7–52.6
10–12	46	12	52.8–58.2	36	16	52.7–59.3
>12	15	4	58.4–65.5	1	0	64.7
Total	394			223		
Max	24			20		

Table 2. Neritic survival equivalent (NSE) and estimated percent of Kemp's ridley sea turtles ≥ age A10 captured by the Coastal Trawl Survey (CTS) (n = 223) and Turtle Trawl Survey (TTS) (n = 394) survey designs, to include limited fishery-dependent (F-D) sampling, through 2019

Survey	Sampling design	Years	A1–A9	A10+	NSE	% A10+
TTS$_1$	Stratified random	2000–2015	207	44	0.91	18
TTS$_2$	Stratified random	2018–2019	27	6	0.92	18
TTS$_3$	F-D; Brunswick, GA	2000	8	1	0.88	11
TTS$_4$	F-D; Charleston, SC	2000–2003	4	0	0.00	0
TTS$_5$	Channel; Charleston, SC	2004–07; 2016–17	2	2	1.00	50
TTS$_6$	Localized; Brunswick, GA	2016–2017	86	7	0.86	8
CTS$_1$	Stratified index	1990–1999	13	2	0.90	13
CTS$_2$	Stratified index	2000–2015	125	25	0.91	17
CTS$_3$	Stratified index	2016–2019	48	10	0.91	17

fied as age 1 (Table 1), 3 of which (all captured in TTS) were smaller than the 21.2 cm SCLnt mean spline reference size. Only one Kemp's ridley sea turtle (also captured in the TTS) was larger (by 0.8 cm SCLnt) than the largest mean spline reference size, and this specimen was in turn extrapolated to be age 24. Maximum age estimated for the largest CTS specimen was 20 yr (64.7 cm SCLnt, Table 1).

Gross size and estimated age distribution were not statistically different between survey captures ($\chi^2 = 0.133$, df = 2, p = 0.936), with 16% of specimens in each survey estimated as ≥10 yr old (Table 1). Except for localized sampling designs within the TTS, and between 1990 and 1999 when only 15 CTS Kemp's ridley sea turtles were captured, size/estimated age structure was consistent across decades within surveys (Table 2). Consequently, NSE scores for non-localized trawl survey designs (i.e. TTS$_{1–2}$ and CTS$_{1–3}$) concisely ranged from 0.90 to 0.92 (Table 2).

Among the 27 TNAs generated with fixed recruitment of 5440 *H* to the NWA annually, survival schedule 24 produced the most similar NSE (0.90, Table 2) to CTS data (0.90 to 0.91, Table 2).

Slightly more conservative survival (i.e. schedule 18) produced the most similar NSE (0.93) to randomized trawling in the TTS (0.91 to 0.92). Alternatively, localized trawling off Brunswick, GA, in 2016–17 produced a lower NSE (0.86) that mirrored survival schedule 17. Sample sizes for other TTS subsets were too limited for emphasis but appear in Table 2. Cluster analysis of TNA inputs and metrics (Table 3) revealed 79% similarity between NSE score and a cluster (94% similarity) formed by abundance and age A0 to A2 survival. Alternatively, the percent of TNA age 10+ was most aligned (76% similarity) with survival during ages A3 to A5.

Table 3. Age-based survival schedule used to generate 27 theoretical neritic assemblages (TNA) under stable annual recruitment, which in turn was used to compute neritic survival equivalent (NSE) scores, the percent of TNA ≥ age A10, and age A1 to A34 abundance. Schedules are sorted by NSE score

Schedule	A0	A1	A2	A3–A5	A6–A34	NSE	% A10+	Abundance
1	0.15	0.18	0.27	0.30	0.70	0	0	199
2	0.15	0.18	0.27	0.30	0.80	0	0	199
3	0.15	0.18	0.27	0.30	0.90	0	0	199
4	0.15	0.18	0.27	0.50	0.70	0	0	220
5	0.15	0.18	0.27	0.50	0.80	0	0	223
6	0.15	0.18	0.27	0.50	0.90	0	0	223
10	0.35	0.38	0.47	0.30	0.70	0	0	1215
19	0.55	0.58	0.67	0.30	0.70	0.69	0	3437
11	0.35	0.38	0.47	0.30	0.80	0.70	0	1224
7	0.15	0.18	0.27	0.70	0.70	0.72	0	261
12	0.35	0.38	0.47	0.30	0.90	0.75	1	1238
20	0.55	0.58	0.67	0.30	0.80	0.76	1	3481
13	0.35	0.38	0.47	0.50	0.70	0.76	1	1442
22	0.55	0.58	0.67	0.50	0.70	0.78	2	4231
8	0.15	0.18	0.27	0.70	0.80	0.80	2	273
16	0.35	0.38	0.47	0.70	0.70	0.81	3	1830
21	0.55	0.58	0.67	0.30	0.90	0.81	3	3567
14	0.35	0.38	0.47	0.50	0.80	0.81	3	1495
25	0.55	0.58	0.67	0.70	0.70	0.82	4	5576
23	0.55	0.58	0.67	0.50	0.80	0.83	4	4448
9	0.15	0.18	0.27	0.70	0.90	0.86	7	297
17	0.35	0.38	0.47	0.70	0.80	0.86	8	1998
15	0.35	0.38	0.47	0.50	0.90	0.88	10	1640
26	0.55	0.58	0.67	0.70	0.80	0.88	10	6222
24	0.55	0.58	0.67	0.50	0.90	0.90	14	5076
18	0.35	0.38	0.47	0.70	0.90	0.93	21	2454
27	0.55	0.58	0.67	0.70	0.90	0.94	26	8023

Eight dynamic models devoid of climate influence were systematically evaluated (Table 4). Model M1 vs. Model 1 established a baseline abundance of 4750 age A1 to A34 Kemp's ridley sea turtles between 1990 and 2015 if 50 K *H* consistently recruited annually (Fig. 2). Higher NSE values (median = 0.87, range = 0.06) were observed with systematic decline in annual proportionate *H* recruitment from the GOM to the NWA (Model M4) than when this proportion remained fixed at 0.15 (Model M2 = 0.84, range = 0.07) or increased annually between 1966 and 2014 (Model M3 = 0.82, range = 0.07). Annual decline in proportionate recruitment also predicted reduced assemblage abundance (median = 25.9 K) compared to fixed (median = 35.4 K) or increasing (median = 49.6 K) proportionate *H* recruitment to the NWA annually (Fig. 2). Systematic decline in annual age A0 to A2 survival produced nominal change in assemblage abundance with (median = 25.3 K, model M6) or without (median = 24.1 K, model M5) corresponding increase in annual age A3 to A5 survival (Fig. 2). Conversely, fixing age A3 to A5 survival at 0.7 annually increased assemblage abundance with (median = 32 .4 K, model M8) and without (median = 35.1 K, model M7) offsetting decline in age A0 to A2 survival (Fig. 2).

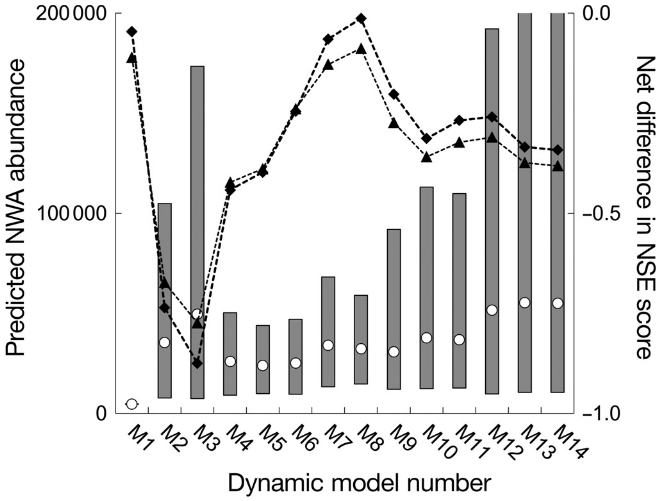

Fig. 2. Median (circle) and inter-annual range (bar) in assemblage abundance (first *y*-axis) between 1990 and 2015 across 14 models (*x*-axis) evaluated with dynamic annual *H* recruitment and annual age-based survival (see Table 4 for parameterization). Best model configuration fit was determined as the least net difference in neritic survival equivalent (NSE) (second *y*-axis) between predicted and observed (Coastal Trawl Survey [CTS] = diamond; Turtle Trawl Survey [TTS] = triangle) data pooled due to low observed sample size for 1990–99, 2000–03, 2004–07, 2008–09, but compared annually during 2010 to 2015

Table 4. Parameterization of 14 dynamic models evaluated for temporal congruency with size/age structure observed in research trawl surveys (Coastal Trawl Survey; Turtle Trawl Survey) in the South Atlantic Bight since 1990. Annual hatchling (*H*) emigration proportion to the Northwest Atlantic Ocean (NWA) (*H* to NWA) was scaled at fixed (M1–M2), at sequential intervals (M3–M8) or negatively correlated with 2 climate-based equations (C, M9-M11; P, M12-M14) as detailed in Section 2. P: Putman eq. *H* given in thousands. Annual survival for ages A0 to A2 was likewise set as either fixed (M1–M4, M7, M9, M12), sequential decline (0.002 yr^{-1}) between 1966 and 2014 (models M5–M6, M8), or with the same range in annual survival negatively correlated with climate-mediated emigration from the Gulf of Mexico to the NWA (models M10–M11, M13–M14). Annual survival for ages A3 to A5 remained fixed except for model M6, when there was a smooth temporal increase (0.002 yr^{-1}), and models M11 and M14, when the same range in survival was positively correlated with climate-mediated emigration. Annual survival remained fixed at 0.9 except for model M6, when a smooth temporal increase of 0.0025 was evaluated between 1966 and 2014

Model	*H* proportion to NWA (years)	Annual survival rate 1966–2014			NSE
		A0–A2	A3–A5	A6–A34	
M1	0.15 (1966–1985)	0.55-0.58-0.67	0.5	0.9	0.90
M2	0.15 (1966–2014)	0.55-0.58-0.67	0.5	0.9	0.84
M3	0.04–0.28 (1966–2014)	0.55-0.58-0.67	0.5	0.9	0.82
M4	0.28–0.04 (1966–2014)	0.55-0.58-0.67	0.5	0.9	0.87
M5	0.28–0.04 (1966–2014)	0.660 to 0.538	0.5	0.9	0.87
M6	0.28–0.04 (1966–2014)	0.660 to 0.538	0.452–0.548	0.852–0.948	0.87
M7	0.28–0.04 (1966–2014)	0.55-0.58-0.67	0.7	0.9	0.90
M8	0.28–0.04 (1966–2014)	0.660 to 0.538	0.7	0.9	0.91
M9	C eq. (1966–2014)	0.55-0.58-0.67	0.7	0.9	0.90
M10	C eq. (1966–2014)	0.660 to 0.538, neg. with C	0.7	0.9	0.89
M11	C eq. (1966–2014)	0.660 to 0.538, neg. with C	0.654–0.750, pos. with C	0.9	0.89
M12	P eq. (1966–2014)	0.55-0.58-0.67	0.7	0.9	0.88
M13	P eq. (1966–2014)	0.660 to 0.538, neg. with P	0.7	0.9	0.88
M14	P eq. (1966–2014)	0.660 to 0.538, neg. with P	0.654–0.750, pos. with C	0.9	0.88

Stepwise regression produced the following climate-based equation (adjusted $r^2 = 0.77$) that approximated a smooth annual decline in H recruitment to the NWA between 1966 (0.28) and 2014 (0.04), and where subscripts denote the observation month of each climate index: Proportionate $H = 0.17041 - (0.1629 \times \text{AMO}_{\text{MAR}}) + (0.01584 \times \text{AMMs,}_{\text{APR}}) - (0.02099 \times \text{AMMs,}_{\text{OCT}}) - (0.00281 \times \text{AMMw,}_{\text{APR}}) + (0.002910 \times \text{AMMw,}_{\text{DEC}})$. Stepwise regression also produced the following climate-based equation (adjusted $r^2 = 1.00$) that reproduced published annual particle emigration rates between 2003 and 2010: Proportionate $H = 17.0202 + (14.8655 \times \text{NAO}_{\text{NOV}}) + (0.8156 \times \text{ENSO}_{\text{JAN–MAR}}) - (15.7219 \times \text{ENSO}_{\text{JUL–SEP}}) - (3.0425 \times \text{AMMs,}_{\text{SEP}}) + (1.31565 \times \text{AMMs,}_{\text{MAR}}) + (0.38172 \times \text{AMMw,}_{\text{OCT}})$.

Among 6 climate-derived annual H recruitment trajectories, lower median abundance (and 16 yr range) was more associated with a smooth temporal decline in proportionate annual H recruitment from the GOM to the NWA (models M9 to M11) than annual proportion predicted for reconstructed passive particle emigration rates (models M12 to M14, Fig. 2). Within these broad constructs, changes in annual survival between ages A0 to A5 produced a small range in median abundance (1990 to 2015) both for smooth temporal decline models (median = 30.8 to 38.8 K) and particle reconstructed models (median = 51.7 to 55.4 K, Fig. 2). Between 1990 and 2015, median NSE scores for climate-derived annual H models spanned 0.88 to 0.90, with corresponding inter-annual range in NSE scores of 0.07 to 0.13.

Net temporal similarity between predicted and observed NSE scores ranged from −0.01 to −0.87 for the CTS (1990 to 2015) and −0.09 to −0.77 for the TTS (2000 to 2015). Model M8 represented the best congruence with CTS and TTS data overall (Fig. 2), but also broadly aligned with temporal variability (Fig. 3). Annual abundance (ages A1 to A34) for model M8 increased from a low of 14 800 in 1990 to a high of 59 157 in 2010 before subsequent annual decline, all of which reflected variable annual H recruitment into the NWA vs. decline in annual neritic survival once in it (Fig. 4).

4. DISCUSSION

Across species populations, the dynamicity of generations reflects the compounded temporal contributions of annual recruitment into, and annual survival among, cohorts within a population. Relative to ecological study, several accepted techniques exist for eva luag annual survival, all of which become increasingly difficult for species with broad spatial and temporal distribution ranges in open aquatic systems. Capture-mark-recapture studies represent perhaps the most cosmopolitan approach to assessing annual survival rates due to relatively low cost and ease of incorporation into physical capture surveys. This approach has been applied across sea turtle species but is often accompanied by wide confidence intervals reflective of limited recaptures (Chaloupka & Limpus 2005, Sasso et al. 2006, Troëng & Chaloupka 2007, Casale et al. 2007). Although of secondary consideration relative to characterizing spatial habitat

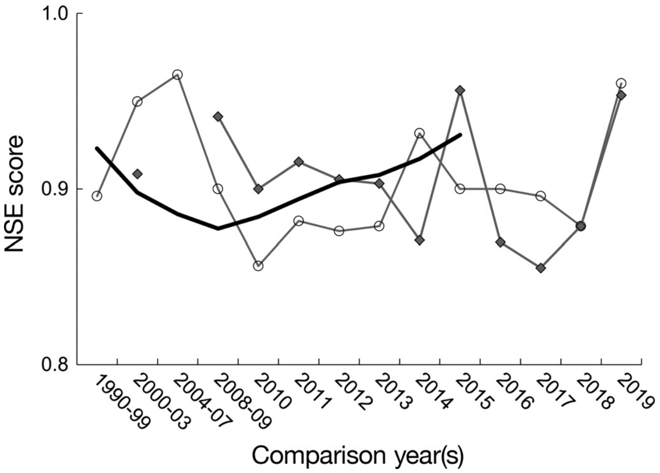

Fig. 3. Temporal oscillation in neritic survival equivalent (NSE) predicted for dynamic Model M8 (thick black line) through 2015 vs. observed for stratified index (Coastal Trawl Survey [CTS], open circle) and random (Turtle Trawl Survey [TTS], filled diamond) trawling

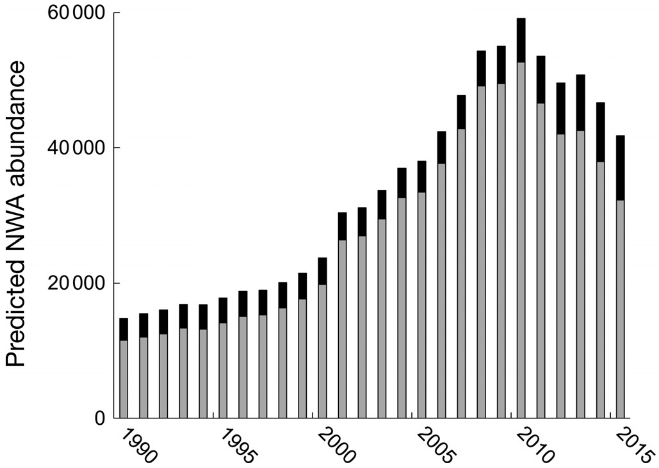

Fig. 4. Annual neritic abundance of Kemp's ridley sea turtles ages A1 to A9 (gray) and age A10+ (black) predicted for the Northwest Atlantic Ocean (NWA) by dynamic Model M8 (see Table 4 for parameterization)

use, telemetry can also provide insight into survival (Sasso & Epperly 2007, Sasso et al. 2011), particularly where transmitters move ashore without evidence of physical detachment (Hays et al. 2003). Akin to recapture studies, though, telemetry survival is inferred from small samples sizes using devices that cease data transmission for many reasons other than host mortality (Hays et al. 2007). Consequently, telemetry methods may bias for low survival rates that radically alter age structure, particularly if applied to younger ages, as we demonstrated with fixed rate modeling. Conversely, catch curve analysis of data collected with robust sampling designs provides incredible insight (and with a high degree of sensitivity) to the combined effect of temporal recruitment and annual survival. Furthermore, variability in NSE scores is relatively less influenced by small sample sizes compared to other catch analysis techniques.

In the present study, minimal temporal variability was suggested for age structure based on size of Kemp's ridley sea turtles captured by research surveys in the SAB over several decades; however, subtle differences were noted among sampling designs within the TTS. In nearshore waters off Brunswick, GA, lower NSE scores stemming from greater capture of smaller/younger specimens were quite similar between fishery-dependent surveys in 2000 and -independent surveys in 2016 and 2017. Based upon recapture by commercial shrimp trawlers, Henwood & Ogren (1987) also identified southern Georgia as a summer/fall foraging area for Kemp's ridley sea turtles originally captured near Cape Canaveral, FL. At least 2, but potentially 6, of 40 Kemp's ridley sea turtles captured near Cape Canaveral, FL (Fig. 3, Henwood & Ogren 1987), were also greater than the Avens et al. (2020) NWA age 10 spline size of 54.1 cm SCLnt, which equates to NSE scores of 0.84 and 0.90, respectively. Henwood & Ogren (1987) also reported tagged Kemp's ridley recaptures off Charleston, SC, but TTS captures near this location were infrequent in both fishery-dependent (2000 to 2003, TTS_4) and shipping channel surveys (TTS_5). Given exponential increase in annual GOM hatchling production since 1985 (NMFS & USFWS 2015), it is difficult to discern if lower NSE scores in these localized survey efforts are more reflective of recruitment of small juveniles or habitat preference. Therefore, this caveat should be taken into consideration when applying the NSE technique to data sets collected in other regions, particularly given aggregation tendency in nearshore coastal and estuarine waters (Christiansen et al. 2016, Coleman et al. 2017, Braun McNeill et al. 2018, Griffin et al. 2019).

Predicted increase in oceanic (and eventually neritic) recruitment of Kemp's ridley sea turtles into the SAB between 1996 and 2017 (Putman et al. 2020a) reflects exponential increase in *H* production in the GOM (NMFS & USFWS 2015). As such, and despite temporal increase in regional encounter rates consistent with greater density, the ratio of older to younger specimens remained stable across decades, to include the 1980s (Henwood & Ogren 1987). As modeled herein, maintenance of consistent size/age structure under increased hatchling production in the GOM required a compensatory reduction in the proportion of annual cohorts emigrating from the GOM to the NWA. Our observed ratios of older to younger cohorts could only be maintained through high annual survival rates at older ages. As such, NWA NSE scores also align with suggestion of limited return of NWA adults to the GOM (see review by Caillouet et al. 2015), since mass remigration would have lowered NSE scores and in turn our suggestion of high neritic survival. Temporal decline in proportionate recruitment from the GOM to the NWA aligned with the decadal periodicity of sea surface temperature change (i.e. AMO and AMM). This association is ecologically plausible given increased occurrence of *Sargassum*, a floating macroalgae recognized as critical habitat for oceanic sea turtles (Witherington et al. 2012), in the western GOM during the warm phase of the Atlantic Multidecadal Oscillation (AMO) (Sanchez-Rubio et al. 2018).

Temporal reduction in the proportion of hatchlings emigrating from the GOM to the NWA bodes well for retention in the GOM for multi-generational population rebuilding, at least during the warm phase of the AMO/AMM. Our findings align with episodically appreciable annual emigration from the GOM to the NWA (Putman et al. 2013, DuBois et al. 2020), which when coupled with high annual survival, bodes well for species persistence. However, proportionate annual *H* emigration predicted by a surrogate equation for Putman et al. (2013) reduced model fit, perhaps reflecting oceanic sea turtles swimming against currents (Putman & Mansfield 2015). Nevertheless, inspired largely by particle simulations, Caillouet (2019, p. 5) sounded the alarm for a better understanding of annual neritic recruitment dynamics for Kemp's ridley sea turtles from the GOM to the NWA, noting that 'to date, additions from immigration and losses from emigration have been ignored' and that population modeling for this species is overdue 'to incorporate metrics of emigration and immigration…to determine whether there is a net loss to the NAO (North Atlantic Ocean).'

Therefore, we emphasize that systematic modeling herein does not support the suggestion of an increase in the proportion of annual emigration, and alternatively suggests a contemporary reduction in the proportion of hatchlings recruiting annually from the GOM to the NWA and generally concurrent with long-term climate forcing.

High annual survival rates for Kemp's ridley sea turtles in the NWA contrast reports from the GOM where extensive modeling of annual survival has been conducted primarily to interpret contemporary trends in annual nest counts (Heppell et al. 2005, Gallaway et al. 2016). Likewise, catch rate increases in North Carolina estuaries (Braun McNeill et al. 2018) may offset concern of abundance decline in Chesapeake Bay based on aerial surveys (Mansfield 2006). Aside from these Mid-Atlantic data sets, we are unaware of other abundance estimates for Kemp's ridley sea turtles in the NWA, let alone annual data compiled for age groups across decades, the significance of which is 2-fold. First, annual abundance scaled for age structure provides a necessary context for evaluating if temporal stranding events have truly increased or have remained proportionately stable (Christiansen et al. 2016, Griffin et al. 2019). Likewise, temporal abundance is also necessary for evaluating the ramifications of elevated incidental take in commercial (Putman et al. 2020b) and recreational (Coleman et al. 2017) fisheries despite the absence of apparent radical change in fishing procedures. Second, as noted by Putman et al. (2020a, p. 513), '… even in regions where predictions of abundance are relatively high (e.g. upwards to 20 000 turtles per 1° of latitude by 1° of longitude) this equates to densities of no more than 1–2 turtles km^{-2}. Such low densities limit the practicality of large-scale oceanic surveys and thus highlight how these simulations could extend the utility of observations obtained over more limited areas.' Alternatively, the combination of age structure modeling to provide context for evaluating size (and inferred age) structure following physical capture is highly informative.

Low density caveats for estimating Kemp's ridley abundance using aerial surveys should not be taken lightly given a recent recommendation for more aerial and less in-water emphasis to monitor loggerhead sea turtles *Caretta caretta* (Linnaeus, 1758) in the NWA (Schroeder et al. 2020). Aerial detection of Kemp's ridley sea turtles may also be problematic given no mention near Brunswick, GA, in June 1996 (Braun & Epperly 1996) despite historical temporal–spatial occurrence (Henwood & Ogren 1987). Conversely, routine winter aerial observation in NC estuaries (Epperly et al. 1995) where increased capture (Braun McNeill et al. 2018) and stranding (Christiansen et al. 2016) is reported may reflect more time spent near the surface in cooler and clearer water (Mansfield 2006). Although catch data may be analyzed for temporal trends, caveats that present hurdles for extrapolating such data to relative abundance, let alone absolute abundance, include the inability to (1) standardize data relative to survey area 'detectability' (Beavers & Ramsey 1998) and (2) capture avoidance (Griffiths et al. 2013). Low explanation of catch rate variance despite extensive parameterization (Arendt et al. 2012a) is also critiqued as proof of poor survey design, yet more likely conveys temporal assemblage change at a far grander scale than *in situ* variable measurement in such surveys. Therefore, in addition to providing a critical regional estimate of temporal abundance for the NWA, we also contend that this estimate should also be the most realistic, given a well-defined size-at-age trajectory for Kemp's ridley sea turtles in the NWA (Avens et al. 2020) upon which our analyses hinged.

Size-at-age data for NWA Kemp's ridley sea turtles reported by Avens et al. (2020) reflected analysis of 432 specimens obtained from Florida to Massachusetts between 1993 and 2017. Although 91% of CTS and TTS captures occurred between central Florida and South Carolina, where only 8% of Avens et al. (2020) specimens originated, the authors did not report differences in growth rates within the NWA. Furthermore, 55% of specimens analyzed by Avens et al. (2020) originated from North Carolina where only 9% of Kemp's ridley sea turtle captures in the present study originated. Greatest GOM vs. NWA difference reported by Avens et al. (2020) was increased prevalence of age 1 and age 2 animals in the NWA, where greater variability in oceanic to neritic transition age than in the GOM was also suggested. Likewise, slower growth rates of age 2 specimens in the NWA vs. the GOM (Avens et al. 2020) may reflect longer duration in oceanic habitats and more stochastic growth (Bjorndal et al. 2003). Differences in GOM vs. NWA stranding size distributions (see Fig. 1 of Avens et al. 2020) also translated into regional differences in age structure among stranding specimens based on mean spline size comparison (see Table 4 of Avens et al. 2020). In the GOM, roughly 10% (~80 specimens >60 cm SCLnt) were likely ≥age 10 vs. just 3% in the NWA (~14 specimens >55 cm SCLnt). These findings suggest differences in cause of stranding, notably greater frequency of small, cold stun strandings in the NWA

(Christiansen et al. 2016, Griffin et al. 2019) but perhaps also greater occurrence of larger, trawling mortalities in the GOM (Gallaway et al. 2016). Consequently, for NSE analysis, our findings also suggest great caution for exclusive use of opportunistically collected specimens vs. those obtained from well-designed sampling surveys.

Extrapolation of the NSE technique to the GOM was beyond the scope of this body of research, but we intend to evaluate reciprocal models in a future manuscript, particularly given suggestion of a climate influence on distribution of Kemp's ridley sea turtles in the NWA. Arendt et al. (2021) demonstrated that a similar climate association with age at neritic recruitment produced multi-decadal oscillation in neritic abundance for a simulated loggerhead sea turtle assemblage in the NWA under fixed annual survival. Oceanic duration of Kemp's ridley sea turtles in the GOM (Avens et al. 2020) is considerably shorter than for loggerhead sea turtles (Bjorndal et al. 2000) in the NWA; however, climate-mediated distribution may still exert strong governance on neritic assemblage structure in the GOM despite most Kemp's ridley sea turtles never leaving that system. To date, climate-mediated governance of annual nest count variability in the GOM has received little attention despite potentially being the driver of density-dependent associations (Kocmoud et al. 2019). Furthermore, population modeling for Kemp's ridlsea turtles in the GOM has predominantly emphasized manipulation of annual survival rates to fit pre-conceived and near-term notions of anthropogenic cause–effect on annual nest counts (Heppell et al. 2005, Gallaway et al. 2016, Kocmoud et al. 2019), rather than these effects superimposed on a background climate signal. Recruitment modeling for the NWA does support the suggestion of increased juvenile abundance in the GOM first raised by Caillouet et al. (2018), but without reciprocal modeling it is not possible to ascertain whether present GOM age structure should be worrisome. Therefore, as a critical first step, we recommend that the age assignment and NSE methodologies described herein be applied to in-water studies that have operated, albeit in mosaic fashion, in the GOM across decades to identify the most appropriate base model for subsequent scenario sleuthing (Witzell & Schmid 2004, Metz & Landry 2016, Lamont & Johnson 2020, Chabot et al. 2021).

Data accessibility statement. Please email the corresponding author to inquire further about accessing data presented herein.

Acknowledgements. Across decades, several hundred personnel representing employees (scientific and otherwise) plus seasonal hires and volunteers greatly contributed to data collection; however, we especially thank 10 apiece with present or former SCDNR affiliation (J. Byrd, C. Evans, J. D. Whitaker, A. Segars, P. Maier, J. Jacobs, R. Schrimpf, M. Schwartz, R. Beatty, E. Wenner) and UGA MAREX affiliation (L. Parker, M. Higgins, H. McIver, L. Gentit, R. Puterbaugh, J. Dickey, B. Fluech, L. Liguori, R. Vendetti, D. Harrington). Funding was provided by NOAA Fisheries via 9 grants to the CTS (NA17FS0053, NA27FS0050, NA47FS-0042, NA77FS0012, NA07FS0004, NA03NMF4350103, NA-06NMF4350021, NA11NMF4350043, and NA16NMF-4350172) and 6 grants to the TTS (NA97FL0375, NA07FL0499, NA03NMF4720281, NA08NMF4720502, NA18NMF4720238, and NA19NMF4720126). Sea turtle activities were authorized by numerous federal permits and/or letters of authorization from multiple NMFS Protected Resources offices (CTS = #1405, #13543, SER-2009-07541, SER-2013-12255; TTS = #1245, #1540, #15566, #195621) as well as state agencies as appropriate (i.e. GADNR #029, #1141, and #21303; FWC MTP #064, #140, #163). We thank E. Hiltz and C. McDonough (SCDNR) as well as anonymous reviewers for editorial improvements to this manuscript. This is South Carolina Department of Natural Resources Contribution 853.

LITERATURE CITED

Arendt M, Boynton J, Schwenter J, Segars A, Byrd J, Whitaker D, Parker L (2012a) Temporal trends (2000–2011) and influences on fishery-independent catch rates for loggerhead sea turtles (*Caretta caretta*) at an important coastal foraging region of the Southeast U.S. Fish Bull 110:470–483

Arendt M, Schwenter J, Segars A, Byrd J and others (2012b) Catch rates and demographics of loggerhead sea turtles (*Caretta caretta*) captured from the Charleston, South Carolina, shipping channel during the period of mandatory use of turtle excluder devices (TEDs). Fish Bull 110: 98–109

Arendt MD, Schwenter J, Owens D, Valverde R (2021) Theoretical modeling and neritic monitoring of loggerhead *Caretta caretta* [Linnaeus, 1758] sea turtle sex ratio in the southeast United States do not substantiate fears of a male-limited population. Glob Change Biol 27:4849–4859

Avens L, Ramizez MD, Hall AG, Snover ML and others (2020) Regional differences in Kemp's ridley sea turtle growth trajectories and expected age at maturation. Mar Ecol Prog Ser 654:143–161

Beavers S, Ramsey F (1998) Detectability analysis in transect surveys. J Wildl Manag 62:948–957

Bjorndal KA, Bolten AB, Martins HR (2000) Somatic growth model of juvenile loggerhead sea turtles *Caretta caretta*: duration of pelagic stage. Mar Ecol Prog Ser 202:265–272

Bjorndal K, Bolten A, Dellinger T, Delgado C, Martins H (2003) Compensatory growth in oceanic loggerhead sea turtles: response to a stochastic environment. Ecology 84: 1237–1249

Bolten A (1999) Techniques for measuring sea turtles. In: Eckert K, Bjorndal K, Abreu-Grobois F, Donnelly M (eds) Research and management techniques for the conservation of sea turtles. IUCN/SSC Marine Turtle Specialist Group Publication No. 4. Consolidated Graphic Communications, Blanchard, PA, p 110–114

Braun J, Epperly S (1996) Aerial surveys for sea turtles in southern Georgia waters, June 1991. Gulf Mex Sci 14: 39–44

Braun McNeill J, Goodman Hall A, Richards PM (2018) Trends in fishery-dependent captures of sea turtles in a western North Atlantic foraging region. Endang Species Res 36:315–324

Caillouet C Jr (2019) Excessive annual numbers of neritic immature Kemp's ridleys may prevent population recovery. Mar Turtle Newsl 158:1–9. www.seaturtle.org/mtn/archives/mtn158/mtn158-1.shtml (accessed 22 February 2021)

Caillouet C Jr, Gallaway B (2020) Kemp's ridley sea turtle emigration and immigration between the Gulf of Mexico and Atlantic Ocean should not be ignored in age-structured population modeling. Mar Turtle Newsl 161:9–14. www.seaturtle.org/mtn/archives/mtn161/mtn161-2.shtml (accessed 1 October 2021)

Caillouet CW, Shaver DJ, Landry AM Jr (2015) Kemp's ridley sea turtle (*Lepidochelys kempii*) head-start and reintroduction to Padre Island National Seashore, Texas. Herpetol Conserv Biol 10:309–377

Caillouet C Jr, Raborn S, Shaver D, Putman N, Gallaway B (2018) Did declining carrying capacity for the Kemp's ridley sea turtle population within the Gulf of Mexico contribute to the nesting setback in 2010–2017? Chelonian Conserv Biol 17:123–133

Carr A (1956) The Windward Road: adventures of a nautralist on remote Caribbean shores. Alfred A. Knopf, New York, NY

Carr A (1980) Some problems of sea turtle ecology. Am Zool 20:489–498

Carreras C, Monzón-Argüello C, López-Jurardo L, Calabuig P and others (2014) Origin and dispersal routes of foreign green and Kemp's ridley turtles in Spanish Atlantic and Mediterranean waters. Amph Rept 35: 73–86

Casale P, Mazaris A, Freggi D, Basso R, Argano R (2007) Survival probabilities of loggerhead sea turtles (*Caretta caretta*) estimated from capture-mark-recapture data in the Mediterranean Sea. Sci Mar 71:365–372

Chabot R, Welsh R, Mott C, Guertin J, Shamblin B, Witherington B (2021) A sea turtle population assessment for Florida's Big Bend, Northeastern Gulf of Mexico. Gulf Caribb Res 32:19–33

Chaloupka M, Limpus C (2005) Estimates of sex- and age-class specific survival probabilities for a southern Great Barrier Reef green sea turtle population. Mar Biol 146: 1251–1261

Christiansen E, Harms C, Godfrey M, Finn S (2016) 2016 North Carolina sea turtle cold stunning event. Proc Int Assoc Aquatic Animal Medicine. 47th Annual IAAAM Meeting and Conference, May 21–26, 2016, Virginia Beach, VA

Coker R (1906) The natural history and cultivation of the diamond-back terrapin, with notes on other forms of turtles. NC Geol Surv Bull 14:1–69. https://files.nc.gov/ncdeq/Energy%20Mineral%20and%20Land%20Resources/Geological%20Survey/Bulletins_NCGS/NCGS_Bulletin_14_Cultivation_of_the_Diamond-Back_Terrapin.pdf (accessed 6 October 2021)

Coleman A, Pitchford J, Baily H, Solangi M (2017) Seasonal movements of immature Kemp's ridley sea turtles (*Lepidochelys kempii*) in the northern Gulf of Mexico. Aquat Conserv 27:253–267

Crowder L, Heppell S (2011) The decline and rise of a sea turtle: how Kemp's ridleys are recovering in the Gulf of Mexico. Solutions 2:67–73

DuBois M, Putman N, Piacenza S (2020) Hurricane frequency and intensity may decrease dispersal of Kemp's ridley sea turtle hatchlings in the Gulf of Mexico. Front Mar Sci 7:301

Epperly S, Braun J, Chester A, Cross F, Merriner J, Tester P (1995) Winter distribution of sea turtles in the vicinity of Cape Hatteras and their interactions with the summer flounder trawl fishery. Bull Mar Sci 56:547–568

Fujisaki I, Hart KM, Bucklin D, Iverson AR and others (2020) Predicting multi-species foraging hotspots for marine turtles in the Gulf of Mexico. Endang Species Res 43: 253–266

Gallaway B, Gazey W, Caillouet C Jr, Plotkin P and others (2016) Development of a Kemp's ridley sea turtle stock assessment model. Gulf Mex Sci 2016:138–157

Gitschlag G (1996) Migration and diving behavior of Kemp's ridley (Garman) sea turtles along the US southeastern Atlantic coast. J Exp Mar Biol Ecol 205:115–135

Gredzens C, Shaver D (2020) Satellite tracking can inform population-level dispersal to foraging grounds of post-nesting Kemp's ridley sea turtles. Front Mar Sci 7:559

Griffin LP, Griffin CR, Finn JT, Prescott RL, Faherty M, Still BM, Danylchuk AJ (2019) Warming seas increase cold-stunning events for Kemp's ridley sea turtles in the northwest Atlantic. PLOS ONE 14:e0211503

Griffiths J, Kelly T, Weeks A (2013) Net-avoidance behavior in platypuses. Aust Mammal 35:245–247

Guo Q, Taper M, Schoenberger M, Brandle J (2005) Spatial-temporal population dynamics across species range: from centre to margin. Oikos 108:47–57

Hardy J (1962) Comments on the Atlantic ridley turtle, *Lepidochelys olivacea kempi*, in the Chesapeake Bay. Chesap Sci 3:217–220

Hart KM, Iverson AR, Fujisaki I, Lamont MM, Bucklin D, Shaver DJ (2018) Sympatry or syntopy? Investigating drivers of distribution and co-occurrence for two imperiled sea turtle species in Gulf of Mexico neritic waters. Ecol Evol 8:12656–12669

Hays GC, Broderick AC, Godley BJ, Luschi P, Nichols WJ (2003) Satellite telemetry suggests high levels of fishing-induced mortality in marine turtles. Mar Ecol Prog Ser 262:305–309

Hays G, Bradshaw C, James M, Lovell P, Sims D (2007) Why do Argos satellite tags deployed on marine animals stop transmitting? J Exp Mar Biol Ecol 349:52–60

Hendrickson J (1980) The ecological strategies of sea turtles. Am Zool 20:597–608

Henwood T, Ogren L (1987) Distribution and migrations of immature Kemp's ridley turtles (*Lepidocheyls kempi*) and green turtles (*Chelonia mydas*) off Florida, Georgia, and South Carolina. Northeast Gulf Sci 9:153–159

Heppell S, Crouse D, Crowder L, Epperly S and others (2005) A population model to estimate recovery time, population size, and management impacts on Kemp's ridley sea turtles. Chelonian Conserv Biol 4:765–771

Hoenig J, Gedamke T (2007) A simple method for estimating survival rate from catch rates from multiple years. Trans Am Fish Soc 136:1245–1251

Kocmoud A, Wang H, Grant W, Gallaway B (2019) Population dynamics of the endangered Kemp's ridley sea turtle following the 2010 oil spill in the Gulf of Mexico: simulation of potential cause-effect relationships. Ecol Model 392:159–178

Lamont MM, Johnson D (2020) Growth rates for immature Kemp's ridley sea turtles from a foraging area in the northern Gulf of Mexico. Mar Ecol Prog Ser 652:145–155

Mansfield K (2006) Sources of mortality, movements, and behavior of sea turtles in Virginia. PhD dissertation, Virginia Institute of Marine Science, College of William and Mary School of Marine Science, Gloucester Point, VA

Manzella S, Caillouet C, Fontane C (1988) Kemp's ridley, *Lepidochelys kempi*, sea turtle head start tag recoveries: distribution, habitat, and method of recovery. Mar Fish Rev 50:24–32

Metz T, Landry A (2016) Trends in Kemp's ridley sea turtle (*Lepidochelys kempii*) relative abundance, distribution, and size composition in nearshore waters of the northwestern Gulf of Mexico. Gulf Mex Sci 33:5

Morreale S (1999) Oceanic migrations of sea turtles. PhD dissertation, Cornell University, Ithaca, NY

Morreale S, Standora S (2005) Western North Atlantic waters: crucial developmental habitat for Kemp's ridley and loggerhead sea turtles. Chelonian Conserv Biol 4:872–882

NMFS & USFWS (National Marine Fisheries Service and U.S. Fish and Wildlife Service) (2015) Kemp's ridley sea turtle (*Lepidochelys kempii*) 5-year review: summary and evaluation. https://repository.library.noaa.gov/view/noaa/17048 (accessed 22 February 2021)

Pritchard P (1969) The survival status of ridley sea turtles in American waters. Biol Conserv 2:13–17

Pritchard P (2007) Evolutionary relationships, osteology, morphology, and zoogeography of ridley sea turtles. In: Plotkin P (ed) Biology and conservation of Ridley Sea turtles. Johns Hopkins University Press, Baltimore, MD, p 45–57

Putman NF, Mansfield KL (2015) Direct evidence of swimming demonstrates active dispersal in the sea turtle 'lost years'. Curr Biol 25:1221–1227

Putman NF, Mansfield KL, He R, Shaver DJ, Verley P (2013) Predicting the distribution of oceanic-stage Kemp's ridley sea turtles. Biol Lett 9:20130345

Putman NF, Seney EE, Verley P, Shaver DJ and others (2020a) Predicted distributions and abundances of the sea turtle 'lost years' in the western North Atlantic Ocean. Ecography 43:506–517

Putman NF, Hawkins J, Gallaway BJ (2020b) Managing fisheries in a world with more sea turtles. Proc R Soc B Biol Sci 287:20200220

Renaud M (1995) Movements and submergence patterns of Kemp's ridley turtles (*Lepidochelys kempii*). J Herpetol 29:370–374

Renaud M, Williams J (2005) Kemp's ridley sea turtle movements and migrations. Chelonian Conserv Biol 4:808–816

Sagarin RD, Gaines SD, Gaylord B (2006) Moving beyond assumptions to understand abundance distributions across the ranges of species. Trends Ecol Evol 21:524–530

Sanchez-Rubio G, Perry H, Franks J, Johnson D (2018) Occurrence of pelagic Sargassum in waters of the U.S. Gulf of Mexico in response to weather-related hydrographic regimes associated with decadal and interannual variability in global climate. Fish Bull 116:93

Sasso C, Epperly S (2006) Seasonal sea turtle mortality risk from forced submergence in bottom trawls. Fish Res 81:86–88

Sasso C, Epperly S (2007) Survival of pelagic juvenile loggerhead turtles in the open ocean. J Wildl Manag 71:1830–1835

Sasso CR, Braun-McNeill J, Avens L, Epperly SP (2006) Effects of transients on estimating survival and population growth in juvenile loggerhead turtles. Mar Ecol Prog Ser 324:287–292

Sasso CR, Epperly SP, Johnson C (2011) Annual survival of loggerhead sea turtles (*Caretta caretta*) nesting in peninsular Florida: a cause for concern. Herpetol Conserv Biol 6:443–448

Schmid J (1996) Marine turtle populations on the east-central coast of Florida: results of tagging studies at Cape Canaveral, Florida, 1986–1991. Fish Bull 93:139–151

Schmid J, Witzell W (2006) Seasonal migrations of immature Kemp's ridley turtles (*Lepidochelys kempii* Garman) along the west coast of Florida. Gulf Mex Sci 2006:28–40

Schmid J, Bolten A, Bjorndal K, Lindberg W, Percival H, Zwick P (2003) Home range and habitat use by Kemp's ridley turtles in west-central Florida. J Wildl Manag 67:196–206

Schroeder B, Bolten A, Hardy R, Keene J and others (2020) Developing and evaluating methods to determine abundance and trends of Northwest Atlantic loggerhead turtles. NOAA Tech Memo NMFS-OPR-67

Seney EE, Landry AM Jr (2011) Movement patterns of immature and adult female Kemp's ridley sea turtles in the northwestern Gulf of Mexico. Mar Ecol Prog Ser 440:241–254

Shaver D, Hart K, Fujisaki I, Rubio C and others (2016) Migratory corridors of adult female Kemp's ridley turtles in the Gulf of Mexico. Biol Conserv 194:158–167

Troëng S, Chaloupka M (2007) Variation in adult annual survival probability and remigration intervals of sea turtles. Mar Biol 151:1721–1730

Willis C, Richardson J, Smart T, Cowan J, Biondo P (2015) Diet composition, feeding strategy, and diet overlap of 3 sciaenids along the southeastern United States. Fish Bull 113:290–301

Witherington B, Hirama S, Hardy R (2012) Young sea turtles of the pelagic *Sargassum*-dominated drift community: habitat use, population density, and threats. Mar Ecol Prog Ser 463:1–22

Witzell W, Schmid J (2004) Immature sea turtles in Gullivan Bay, Ten Thousand Islands, southwest Florida. Gulf Mex Sci 22:5

Witzell W, Geis A, Schmid J, Wibbels T (2005) Sex ratio of immature Kemp's ridley turtles (*Lepidocheyls kempi*) from Gullivan Bay, Ten Thousand Islands, southwest Florida. J Mar Biol Assoc UK 85:205–208

Wyneken J, Epperly S, Higgins B, McMichael E, Merigo C, Flanagan J (2010) PIT tag migration in sea turtle flippers. Herp Rev 41:448–454

Appendix. Table A1. Glossary of important terms and acronyms. SCDNR: South Carolina Department of Natural Resource

Term or Acronym	Description	Distinction
GOM	Gulf of Mexico	Epicenter for Kemp's ridley nesting
NWA	Northwest Atlantic Ocean	Ocean basin where trawl surveys were conducted
SAB	South Atlantic Bight	Geographic region of NWA where trawl surveys occurred
CTS	Coastal Trawl Survey	SCDNR survey spanning NC to FL, multi-season, first Kemp's ridley capture in 1990
TTS	Turtle Trawl Survey	SCDNR survey spanning SC to FL, single-season, first Kemp's ridley capture in 2000
SCLnt	Straight carapace length (cm), maximum	Standardized survey sea turtle size measurement
Hatchling, *H*	Cohort abundance	Hatchling production data (1966–2014) extensively modeled for this species
Emigration, *E*	Departure from area of origin	Proportion of annual *H* exiting the GOM
Recruitment, *R*	Arrival into a new area	Proportion of annual *H* entering the NWA
Survival, *S*	Annual survival	Multiplier used to reduce assemblage abundance annually, only offset by *R*
A	Age, sequential	Assigned for each Kemp's ridley based on size (SCLnt) at capture
Q	Age group ratio	Ratio of older to younger animals, base term for the inverse power function
t	Mean age difference between 2 groups	Denominator of exponent term for the inverse power function
NSE	Neritic survival equivalent	Comprehensive measure of assemblage change reflecting annual *S* and *R*
TNA	Theoretical neritic assemblage	Age-structured population constructed using fixed survival and annual *H* abundance
Model(-s, -ing); *M*	Exploratory data analysis	Age-structure projection to evaluate relative importance of a suite of parameters
Configuration(s)	Parameterization	Specific values for *H* abundance and/or age-based survival rates used for modeling
Trajectory	Directionality of temporal change	Stable, decreasing, or increasing in change in *R* or *S* between 1966 and 2014
AMO	Atlantic Multidecadal Oscillation	Associated with *Sargassum* retention in western GOM and sea turtle nesting in FL
AMMs	Atlantic Meridional Mode, surface temperature	Associated with *Sargassum* retention in western GOM
AMMw	Atlantic Meridional Mode, wind forcing	Associated with *Sargassum* retention in western GOM
NAO	North Atlantic Oscillation	Associated with *Sargassum* retention in western GOM and sea turtle nesting in FL
ENSO	El Niño-Southern Ocean Oscillation	Associated with *Sargassum* retention in western GOM, originates in Pacific Ocean

Editorial responsibility: Matthew Godfrey,
Beaufort, North Carolina, USA
Reviewed by: M. D. Ramirez, C. W. Caillouet Jr. and
2 anonymous referees

Submitted: June 24, 2021
Accepted: April 25, 2022
Proofs received from author(s): June 29, 2022